Properties of *n*-Eicosane-Loaded Silk Fibroin-Chitosan Microcapsules

Guldemet Basal,[1] Senem Sirin Deveci,[1] Dilek Yalcin,[2] Oguz Bayraktar[2]

[1]*Department of Textile Engineering, Ege University, Faculty of Engineering, 35100, Bornova-Izmir, Turkey*
[2]*Department of Chemical Engineering, Izmir Institute of Technology, Gülbahçe Köyü, 35430, Urla-Izmir, Turkey*

Received 21 December 2009; accepted 23 October 2010
DOI 10.1002/app.33651
Published online 10 March 2011 in Wiley Online Library (wileyonlinelibrary.com).

ABSTRACT: PCM microcapsules containing *n*-eicosane were prepared by complex coacervation of silk fibroin (SF) and chitosan (CHI). Chemical characterization of microcapsules was carried out using Fourier-transform infrared (FT-IR) spectroscopy. Thermal properties and thermal stability of microencapsulated *n*-eicosane were determined by differential scanning calorimetry (DSC) and thermal gravimetric analysis (TGA). FTIR spectra confirmed the encapsulation of *n*-eicosane within the microcapsules. Results from thermal analyses showed that microcapsules consisted of an average of 45.7 wt % *n*-eicosane, and had a thermal energy storage and release capacity of about 93.04 J/g and 89.68 J/g, respectively. © 2011 Wiley Periodicals, Inc. J Appl Polym Sci 121: 1885–1889, 2011

Key words: microcapsule; PCM; silk fibroin; chitosan; *n*-eicosane

INTRODUCTION

PCMs are substances which are capable of storing or releasing large amounts of energy as they melt and solidify at certain temperatures.[1,2] There are large numbers of phase change materials that melt and solidify at a wide range of temperatures, making them attractive in a number of applications including solar and nuclear heat storage systems, packed bed heat exchangers, and thermoregulated textiles.[3] Initially, PCM technology was utilized in late 1970s to the early 1980s by the US National Aeronautics and Space Administration (NASA) to protect delicate instruments in space from large temperature extremes.[4] NASA utilized a variety of PCMs including lithium chloride for mainly heat management of electronics, telecommunications, and microprocessor equipment. For classical textile applications PCMs came into use in the late 1980s. Yvonne G. Bryant and David P. Colvin issued a patent demonstrating the feasibility of incorporating PCMs within textile fibers in 1994.[5] Today the PCMs with a phase change temperature range just above and just below human skin temperature are being used in thermoregulated textiles or heat storage textiles. These textiles absorb heat from environment when surrounding temperature is higher than their phase change temperature and they release heat when temperature is lower than that value. By doing so, they keep the wearer in a state of thermophysiological comfort under the widest possible range of ambient conditions and physical activity levels.[6–10] Especially paraffin waxes or linear chain hydrocarbons are preferred for thermoregulated textiles since they have high heat storage capacities and their phase transition temperature lie in the range of comfort temperature of human body.[2,3,10,11]

The main problem with PCM materials including paraffins is their low thermal conductivity, which limits the thermal power that can be extracted from them.[12] One way of solving this problem is the inclusion of metal nanoparticles into PCMs.[13,14] Another way is encapsulating the material into relatively small capsules through microencapsulation process.[15] As a result of microencapsulation, reactivity of the PCM materials with the outside environment is reduced and the heat transfer area is increased.

For encapsulation of PCM materials numerous microencapsulation techniques can be used including *in situ* polymerization, interfacial polycondensation, suspension polymerization, and complex coacervation. Complex coacervation, one of the oldest and perhaps the most widely used method of microencapsulation, involves the formation of a continuous capsule wall around a suspended core. The capsule wall is formed of two oppositely charged polymers in an aqueous solution, that interact together to form a coacervate polymer which wraps around the core to form the wall. After wall formation, the capsule walls are crosslinked.[16,17] Traditionally, the complex coacervation technique entails the capsulation of lipophilic water-immiscible

Correspondence to: G. Basal (guldemet.basal@ege.edu.tr).
Contract grant sponsor: Ege University Research Foundation; contract grant number: 08-MUH-042.

materials, but it is also possible to encapsulate some water-soluble actives using this technique by forming a water-in-oil (W/O) emulsion.[18]

In our previous work[19] we prepared PCM microcapsules by complex coacervation of silk fibroin (SF) and chitosan (CHI) and examined the effects of polymer ratio, crosslinking agent, and PCM (*n*-eicosane) content on the surface morphology and size distribution of microcapsules, and the microencapsulation efficiency. In this study, we investigated chemical characteristics, melting and crystallization properties, and thermal stability of the microcapsules by utilizing FTIR, DSC, and TGA.

EXPERIMENTAL

Materials

n-Eicosane with a purity of above 98% was supplied by Merck, Germany and was used as microcapsule's core. Span-20, an emulsifier, was purchased from Fluka, Singapore. Silk fibroin (SF) with a purity of 99% and in the form of superfine silk powder (the particle diameter $\leq$ 5 μm) was supplied from Wuxi Smiss Tech. Co. Ltd., China. Low molecular weight chitosan with a 75–85% deacetylation degree and a viscosity of maximum $\sim$ 200 cps was purchased from Σ-Aldrich Chemicals. Acetic acid (%100), which was used to dissolve the chitosan, was supplied by Merck. Glutaraldehyde (50% water solution) was obtained from Fluka, Switzerland and used for the crosslinking of capsule walls.

Preparation of SF-CHI coacervate microcapsules

Phase change material incorporated silk fibroin-chitosan microcapsules were manufactured through the complex coacervation of silk fibroin and chitosan, described in our previous study.[19] To obtain chitosan solution 0.21 g of chitosan was added to the 2% (v/v) acetic acid aqueous solution and the temperature of solution was raised to 50°C. The dissolution was occurred under magnetic stirring for about 15 min. Silk fibroin solution was prepared by means of Ajisawa method. First, pure silk powder was dissolved in a mixed triad solvent of '$CaCl_2{\cdot}2H_2O$'/H_2O/EtOH with a 1:8:2*M* ratio at 78°C and 125 rpm stirring speed for about 2 h. Then, the solution was dialyzed using cellulose tubular membranes in distilled water for minimum three days at $\sim$ 4°C.

To form an oil-in-water system 6.75 g melted *n*-eicosane was emulsified into 230 mL of 1.8%(w/v) silk fibroin solution by stirring at 300 rpm for 20 min. To obtain a stable emulsion, 0.68 g Span-20 was added to the dispersed phase. During the homogenization process, 220 mL chitosan solution was added drop-by-drop a dropping funnel. The ratio of silk fibroin to chitosan was 20. After the addition of chitosan, the pH of mixture was adjusted to 5.2 $\times$ 5*M* NaOH solution to attain the maximum coacervation. Agitation was continued for almost 1 h. The temperature was maintained at 50°C throughout emulsification. The next step was hardening of microcapsules, which was accomplish by adding 8.17 mL of gluteraldehyde solution (50 wt %) dropwise to the mixture. The concentration of gluteraldehyde in the final solution was 0.9%. To complete the crosslinking reaction stirring was continued for about 2 to 3 h. The final step was isolation of microcapsules. The temperature of solution was reduced to the room condition. Then, the suspension was filtered and the microcapsules were dried overnight.

Characterization of microcapsules

The surface functional groups of the core materials and microcapsules were analyzed by a FTIR (Digilab FTS 3000 Mx) spectrophotometer with a scanning number of 50 and the resolution of 4 cm^{-1}. The thermal properties of the microcapsules were examined using a dynamic differential scanning calorimeter (TA Instrument Q10) at a heating or cooling rate of 2°C/min under a nitrogen atmosphere with the weights of the samples being about 10 mg. The thermal stability of the microcapsules and *n*-eicosane was determined using a Schimadzu DSC-50 thermal gravimetric analyzer from 25 to 550°C at a heating rate of 10°C/min.

RESULTS AND DISCUSSION

Morphology and particle size

Our previous study[19] showed that microcapsules obtained through this method are regularly spherical with a fairly uniform structure [Fig. 1(a)], and they have a particle size ranging from 8 to 38 μm. An interesting finding was that the wall of microcapsules consists of two distinctive layers, a rigid layer covered by a sponge like layer [Fig. 1(b)].

Chemical structure of microcapsules

To identify the microcapsule composition, FTIR, one of the most widely used analytical tools for chemical structures of organic compounds, was used. FTIR spectra of *n*-eicosane, silk fibroin, chitosan, SF/CHI microcapsules containing *n*-eicosane and the polymer wall in the range 4000–400 cm^{-1} were recorded and presented in Figure 2.

FTIR spectrum [Fig. 2(a)] of chitosan exhibited characteristic absorption bands. The absorption band at 3448 corresponds to hydroxyl group,[20] at 1080 corresponds to the skeletal vibrations involving the

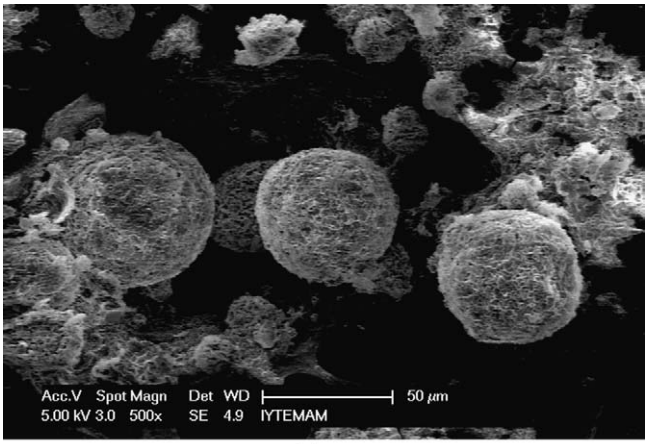

(a)

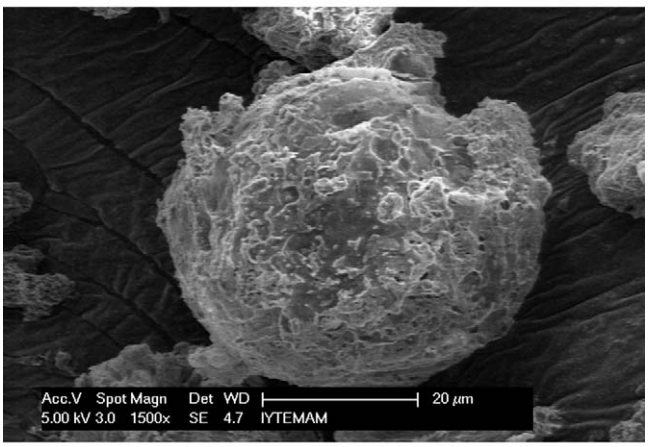

(b)

Figure 1 (a) SF/CHI microcapsules (b) two layer structure of a cracked microcapsule obtained through nitrogen treatment.

CO stretching, which is characteristic of chitosan saccharide structure,[21] at 1653 cm^{-1} corresponds to C=O stretching in amide group (amide I vibration),[21,22] at 1560 cm^{-1} corresponds to *N*—H bending in amide group, (amide II vibration)[21] and at 1595 cm^{-1} corresponds to *N*—H bending in nonacetylated 2-aminoglucose primary amine.[21,22,23]

Two major secondary structures of silk fibroin, Silk I and II, are well known in the literature.[24,25] Silk I is a metastable conformation composed of random coils and α-helix structures. Silk II is primarily composed of antiparallel β-sheets. FTIR spectrum of pure silk fibroin powder used as starting material to obtain aqueous fibroin solution was given in Figure 2(d). As expected, The FTIR spectrum of pure silk fibroin powder confirmed the β-sheet conformation showing typical amide absorption bands at 1636 cm^{-1} (Amide I), 1526 cm^{-1} (Amide II), and 1231 cm^{-1} (Amide III) [Fig. 2(d)]. In the preparation of microcapsules, silk fibroin molecules are strongly solvated in the $CaCl_2$ ternary solvent, aqueous fibroin solutions used in the preparation of microcapsules are metastable (Silk I) in the dialyzed solution. Silk I can be converted to Silk II by heating, mechanical deformation, alcohol treatments, blending, or complexation with another biopolymer.[26–30]

The FTIR spectrum [Fig. 2(d)] of silk fibroin powder (indicating Silk II structure) used as a finger print to reveal the conformational changes of fibroin (Silk I structure) due to the microcapsule wall material formation with chitosan. The appearance of strong and broad peaks of SF-CHI microcapsules and wall material [Fig. 2(b,c)] at 1240 cm^{-1} represented that the dominant conformation was silk I, when compared to the β-sheet dominant conformation of control SF powder [Fig. 2(d)] which showed 1231 cm^{-1} absorption band of the Silk II conformation. For FTIR spectra of SF-CHI microcapsules and wall material [Fig. 2(b,c)] the appearance of a peak at 1543 cm^{-1} and small shoulder in the region of 1620–1631 cm^{-1} revealed the presence of both Silk I and II structures, respectively. The presence of β-sheets (Silk II) may be attributed to hydrogen bonds and electrostatic interactions between SF and CHI molecules. Intermolecular hydrogen bond could be observed by the appearance of a peak at 3294 cm^{-1} [Fig. 2(c)]. In general, blending or complexation with another biopolymer caused SF molecule to change its secondary structure from Silk I to Silk II. Our findings are in accordance with those reported for similar systems in the literature.[27–31] The peak (1062 cm^{-1}) associated with aliphatic amino groups is attributed to CHI.

The absorption peaks at 1472 and 717 cm^{-1} in the spectra of *n*-eicosane and SF/CHI microcapsules containing *n*-eicosane were attributed to the aliphatic C—H stretching vibration and the in-plane rocking vibration of CH_2 group, respectively, [Fig. 2(e)]. The FTIR spectrum of the wall material did not show

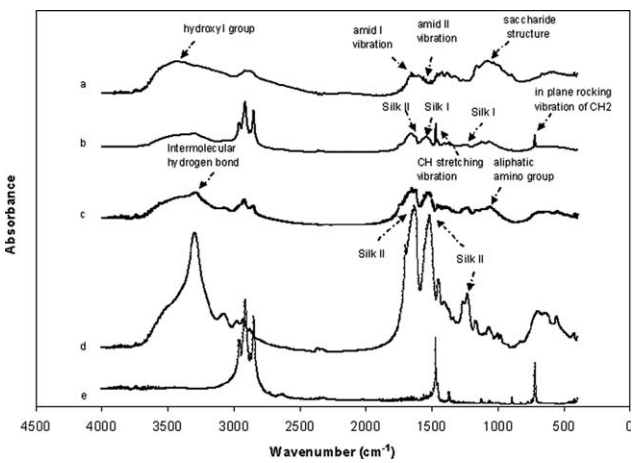

Figure 2 FTIR spectra of (a) chitosan B, (b) *n*-eicosane containing microcapsules, (c) wall, (d) silk-fibroin, and (e) *n*-eicosane.

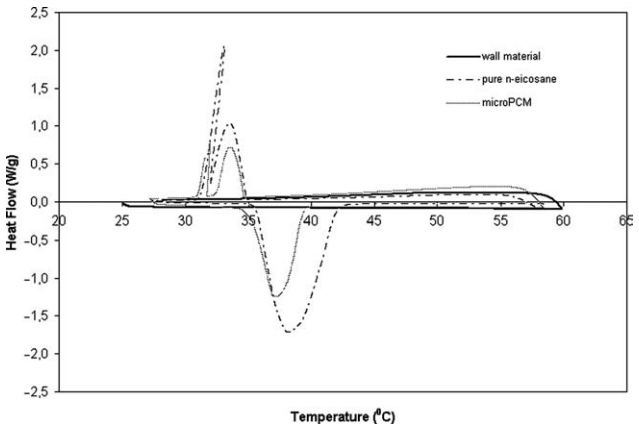

Figure 3 DSC curves of pure *n*-eicosane, microPCM, and wall material.

these specific peaks [Fig. 2(c)]. This proves that *n*-eicosane was successfully microencapsulated.

Thermal characteristics of microcapsules

Phase change behaviors

The phase change enthalpies and phase change temperatures of pure *n*-eicosane, microPCM, and wall material were determined by DSC. The heating and cooling thermograms are shown in Figure 3 and Table I. From the DSC heating thermograms, a single peak can be observed for pure *n*-eicosane and microcapsule containing *n*-eicosane. The cooling thermogram, on the other hand, demonstrates two peaks, which are attributed to two crystallization temperatures (i.e., α-and β-crystalphase) of *n*-eicosane. The DSC thermograms of the wall material, on the other hand, did not show any subsequent variation of heat flow signal during the heating and the cooling process. This clearly shows that *n*-eicosane was successfully encapsulated inside the silk fibroin/chitosan microcapsules. The latent heats of melting and freezing of microPCMs were measured as 93.04 and 89.68 J/g, respectively. The *n*-eicosane content in the microcapsules according to the DSC measurement was 45.7 wt %. The encapsulated PCM ratio affects the thermal capacity of microcapsules; however, there should be a balance between the thermal capacity and the stability of microcapsules. In case of high *n*-eicosane content, the capsule wall might be too thin to sustain great volume changes during multiple thermal cycles.

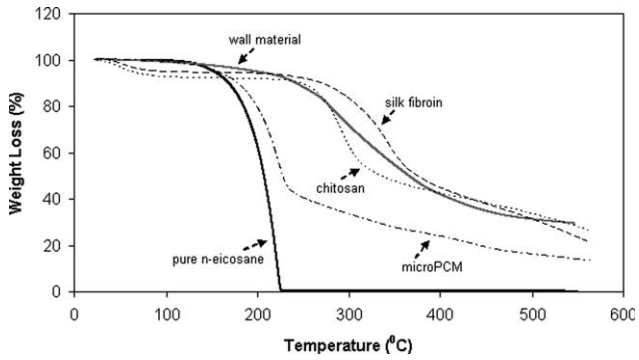

Figure 4 TGA thermograms of pure *n*-eicosane, microPCM, and wall material.

In the experiments, PCM content of microcapsules was calculated according to following equation.

$$\mathrm{PCM(wt\%)} = \frac{\Delta H_{m,\mathrm{microPCM}} + \Delta H_{c,\mathrm{microPCM}}}{\Delta H_{m,\mathrm{PCM}} + \Delta H_{c,\mathrm{PCM}}} \times 100 \quad (1)$$

where $\Delta H_{\mathrm{microPCM}}$, ΔH_{PCM} are measured enthalpies of microcapsules containing *n*-eicosane and *n*-eicosane itself, respectively.

Thermal stabilities

Figure 4 shows the TGA thermograms for a representative set of microencapsulated PCMs and wall material with respect to those of silk fibroin and of chitosan. The collected data are expressed as weight loss (%) and temperature (25–550°C). Initial weight losses in all thermograms below 120°C can be ascribed to the evaporation of adsorbed and bound water. Weight loss in the range of 240–550°C on the TGA curves can be assigned to the thermal decomposition of organic macromolecules.

The thermogram of microencapsulated PCM exhibits two distinct weight loss steps. To analyze each degradation steps TGA curves of wall material, *n*-eicosane, silk fibroin, and chitosan as the constituents of wall material were taken into consideration. According to data, pure *n*-eicosane lost 5% of its weight at 150°C and total weight loss occurred at 225°C. The first step weight loss of microcapsules on TGA curves below

TABLE I
Phase Change Properties and Thermal Stabilities of Pure n-Eicosane and the MicroPCM

Sample No	Sample type	T_m	ΔH_m (J/g)	T_c A	T_c ß	ΔH_c (J/g)	Encapsulation ratio (%)
1	Pure n-eicosane	38.17	203.7	33.37	33.08	215.95	100
2	microPCM	37	93.04	33.52	31.93	89.68	45.67

240°C is mainly attributed to the diffusion of core material (*n*-eicosane) and its decomposition. When the temperature is approximately up to 240°C, the wall material begins to decompose gradually. The residual materials are decomposed further above 240°C, the weight loss rates increase. The first degradation step involving the core material (40 wt %) is evident at higher temperatures. It is worth noting that the weight loss temperature of microencapsulated *n*-eicosane is higher than that of the bulk. This is due to the coacervate wall material as a result of increased hydrogen bonding interaction between silk fibroin and chitosan and to the shielding effect of this wall material. Totally, 5% weight loss for wall material took place at 200°C. Similar to micro PCMs the wall material weight loss starts at 240°C and continues up to 500°C. The weight loss from 240 to 500°C may contribute to the decomposition of coacervate structure between chitosan and silk fibroin.

TGA of chitosan showed that weight loss starts at 240°C and continues up to 400°C during which there was 50% weight loss due to the degradation of chitosan. The decomposition of pure chitosan was ascribed to a complex process including dehydration of the saccharide rings, depolymerization and decomposition of the acetylated and deacetylated units of polymer. TGA of chitosan shows a narrow degradation with a maximum degradation temperature at 310°C while wall material has a broad degradation pattern with maximum degradation at 350°C. SF started decomposition at about 240°C and continued up to 400°C. The thermal decomposition was caused by the disintegration of intermolecular interaction and partial breakage of the molecular structure. Silk fibroin also shows narrower degradation pattern similar to chitosan but with a maximum degradation temperature at 330°C.

These results also indicate the successful encapsulation of core material inside the silk fibroin/chitosan microcapsules.

CONCLUSIONS

The microPCMs with *n*-eicosane core were synthesized by complex coacervation of silk fibroin (SF) and chitosan (CHI). The FTIR spectra, DSC and TGA curves confirmed that *n*-eicosane was successfully encapsulated within the SF/CHI wall. The latent heats of melting and freezing of SF/CHI microcapsules were determined as 93.04 and 89.68 J/g by DSC analysis. The average *n*-eicosane content of microcapsules was 45.7 wt %.

Even though this study proved that it is possible to produce microPCMs by complex coacervation of silk fibroin (SF) and chitosan (CHI) further studies are required to assess the suitability of these microcapsules for textile applications. Particularly, the determination of the mechanical strength of the microcapsule wall is very important since the fixation of microcapsules into textile material and their durability greatly depend on it.

References

1. Farid, M. M.; Khudhair, A. M.; Razack, S. A.; Al-Hallaj, S. Energy Conversion Manage 2004, 45, 1597.
2. Parys, M. V. In Functional Coatings by Polymer Microencapsulation; Ghosh, S. K., Ed.; Wiley-VCH: Weinheim, 2006; Chapter 7.
3. Mondal, S. Appl Thermal Eng 2008, 28, 1536.
4. Nelson, G. Int J Pharm 2002, 242, 55.
5. Mansfield, R. G. Textile World 2004, 3.
6. Thakare, A. M.; Sangwan, A.; Yadav, S. Man Made Textiles India 2005, 48, 239.
7. Zhang, X. X. In Smart Fibres, Fabrics and Clothing; Tao, X. M., Ed.; C. R. C. Press: Boca Raton, FL, 2001;Chapter 3.
8. Ying, B.; Kwok, Y. L.; Li, Y.; Yeung, C. Y.; Song, Q. W. Int J Cloth Sci Technol 2004, 16, 84.
9. Bendkowska, W.; Tysiak, J.; Grabowski, L; Blejzyk, A. Int J Cloth Sci Technol 2005, 17, 209.
10. Ying, B.; Kwok, Y. L.; Li, Y.; Zhu, Q. Y.; Yeung, C. Y. Polym Test 2004, 23, 541.
11. Younsook, S.; Dong-Il, Y.; Kyunghee, S. J Appl Polym Sci 2005, 96, 2005.
12. Zalba, B.; Marin, J.; Cabeza, L.; Mehling, H. Appl Ther Eng 2003, 23, 251.
13. Zeng, J.; Sun, L.; Xu, F.; Tan, Z.; Zhang, Z.; Zhang, J.; Zhang, T. J Thermal Anal Calorimetry 2007, 87, 369.
14. Ho, C. J.; Gao, Y. J. Int Commun Heat Mass Transfer 2009, 36, 467.
15. Kenisarin, M.; Mahkamov, K. Renewable Sustainable Energy Rev 2007, 1913, 11.
16. Thies, C. In Microencapsulation: Methods and Industrial Applications; Benita, S., Ed.; Marcel Dekker Inc: New York, 1996; Chapter 1.
17. Dombrow, M. In Micro-Capsules and Nanoparticles in Medicine and Pharmacy: Overview and Introduction; Dombrow, M., Ed.; CRC Press: Boca Raton, 1992.
18. Sales, B.; Palmer, D. Speciality Chem Mag 2008, 3, 26.
19. Deveci, S. S.; Basal, G. Colloid Polym Sci 2009, 287, 1455.
20. Bhumkar, D. R.; Pokharkar, V. B. AAPS PharmSciTech 2006, 7, E50.
21. Pawlak, A.; Mucha, M. Thermochim Acta 2003, 396, 153.
22. Gierszewska-Drużyńska, M.; Ostrowska-Czubenko, J. Progress on Chemistry and Application of Chitin and Its Derivatives; Jaworska, M. M., Ed.; Polish Chitin Society: Łódź, 2010, Vol. XV.
23. Umemura, K.; Kawai, S. J Appl Polym Sci 2008, 104, 2481.
24. Hu, X.; Kaplan, D.; Cebe, P. Macromolecules 2006, 39, 6161.
25. Yamada, K.; Tsuboi, Y.; Itaya, A. Thin Solid Films 2003, 440, 208.
26. Taketani, I.; Nakayama, S.; Nagare, S.; Senna, M. Appl Surf Sci 2005, 244, 623.
27. Nogueira, G. M.; Swiston, A. J.; Beppu, M. M.; Rubner, M. F. Langmuir 2010, 26, 8953.
28. Chen, X.; Li, W.; Zhong, W.; Lu, Y.; Yu, T. J Appl Polym Sci 1997, 65, 2257.
29. Malay, O.; Bayraktar, O.; Batigun, A. Int J Biol Macromol 2007, 40, 38.
30. Malay, O.; Yalcin, D.; Batigun, A.; Bayraktar, O. J Thermal Analy Calorimetry 2008, 94, 749.
31. Chen, X.; Li, W.; Yu, T. J. Polym Sci, Part B: Polym Phys 1997, 35, 2293.